Cleaner synthesis of silylated clay minerals for the durable recovery of ions (Co2+ and Sr2+) from aqueous solutions

Thomas Thiebault, Jocelyne Brendlé, Grégoire Auge, Lionel Limousy

Separations

Cleaner synthesis of silylated clay minerals for the durable recovery of ions (Co2+ and Sr2+) from aqueous solutions

Thomas Thiebault, Jocelyne Brendlé, Grégoire Augé, and Lionel Limousy

Ind. Eng. Chem. Res., **Just Accepted Manuscript** • DOI: 10.1021/acs.iecr.9b06118 • Publication Date (Web): 15 Jan 2020

Cleaner synthesis of silylated clay minerals for the durable recovery of ions (Co^{2+} and Sr^{2+}) from aqueous solutions

Thomas Thiebault[†,‡,§,*], *Jocelyne Brendlé*[†,‡], *Grégoire Augé*[Φ] *and Lionel Limousy*[†,‡]

[†]Université de Haute-Alsace; IS2M, CNRS, UMR 7361, 3b Rue Alfred Werner, F68100, Mulhouse, France

[‡]Université de Strasbourg, France

[§]EPHE, PSL University, UMR 7619 METIS (SU, CNRS, EPHE), 4 Place Jussieu, F75005, Paris, France

[Φ]ONET Technologies, 36 Boulevard de l'Océan, CS 20280, 13258, Marseille Cedex 09, France

* To whom correspondence should be addressed. E-mail: thomas.thiebault@ephe.psl.eu

Phone: +33 (0) 1 44 27 59 97

ABSTRACT

The impact of the synthesis conditions on the structure and the radionuclide adsorption capacity of silylated clay minerals were evaluated in this study. Two green solvents were selected in this work, Phenoxypropanol and Glycerol respectively, and various synthesis temperatures (30, 60 and 90°C) were tested for the preparation of 3-aminopropyltriethoxysilane (APTES) functionalized Laponites®. The resulted adsorbents exhibit various extent and location of the grafting reaction as a function of the used solvent and temperature. These modifications of the reactivity of the materials also impact adsorption and desorption properties of Co^{2+} and Sr^{2+}. Whereas the two ions are well-adsorbed whatever the synthesis conditions and even in bi-solute experiments, the adsorption capacity is not systematically proportional to the amount of loaded APTES, highlighting the specific impact of the synthesis conditions. Finally, the very limited desorption in saline solutions suggests that the synthetized adsorbents display suitable properties for the removal of radionuclides from aqueous solutions.

INTRODUCTION

Clay minerals are renowned for a while as appropriate materials for the adsorption of various contaminants such as pharmaceuticals, pesticides, inorganic cations and radionuclides.[1–5] However, raw clay minerals may present a limited selectivity and capacity for several adsorbates, especially non cationic ones.[6–8] To overcome these limitations, the use of organic moieties such as surfactants and silylating agents was suggested for the organo-modification of clay minerals.[9–12]

Specifically, the silylation of clay minerals through the grafting of organoalkoxysilanes has raised the interest of the scientific community due to the potential of the resulted compounds for the removal of various contaminants.[13–17] One of the main advantage of such treatment is the durable immobilization of organic moieties after the grafting reaction (i.e. covalent bonding), resulted in stable adsorbents in a wide range of applications unlike surfactant modified clay minerals.[18,19] Moreover, the use of silylated clay minerals (or organic-inorganic hybrids having a saponite or a talc like-structure) for the removal of inorganic cations such as heavy metals and radionuclides was successfully tested.[20–24]

As the ion-exchange properties of clay minerals are maintained during the grafting process, multi-functional compounds are therefore formed enabling the removal of pollutants both by ion-exchange and through binding or chelating with the organic moieties.

Among these contaminants, radionuclides such as ^{60}Co and ^{90}Sr are considered as particularly hazardous due to their important solubility, long half-lives (5.27 and 28.8 years, respectively) and significant occurrences in radioactive wastes.[25,26] Currently, the decontamination of these wastes, mostly generated by nuclear power plant operations, is of high concern due to their chemical hazard and complexity.[27,28] Hence, a suitable removal solution should be specific, capacitive and irreversible for the targeted contaminants. A particular interest of such hybrid materials concerns the fact that they are easy to entrap in glass (possibility to form Si-O-Si covalent bonds). It means that they are good candidates for radionuclide immobilization in conventional matrix used for radioactive waste conditioning.

Adsorption represents an appropriate way for the management of radionuclides from radioactive wastes if the selected adsorbent displays appropriate adsorption properties

and reasonable synthesis cost.[29,30] Moreover, the synthesis of the adsorbent should be both cheap and sustainable by using a new generation of alternative solvents,[31] fulfilling the criteria of "green chemistry",[32] and optimizing the synthesis temperature in order to maximize the adsorption properties of the resulted adsorbents.[33,34]

In this context, the main objective of this work is to investigate the influence of the synthesis conditions (i.e. solvent and temperature) on the structure of silylated clay minerals and their removal properties of Sr^{2+} and Co^{2+}. The starting clay minerals used in this study was a synthetic hectorite (Laponite® RD), grafted with 3-aminopropyltriethoxysilane in two biomass derived solvents, Glycerol (Gly) and Phenoxypropanol (Phe), at three different temperatures (i.e., 30, 60 and 90°C). The adsorption isotherms of stable isotopes of ^{60}Co and ^{90}Sr (*i.e.* ^{59}Co and ^{88}Sr, respectively) were performed in single solute and binary mixtures, as well as desorption experiments which were conducted in various types of saline solutions.

EXPERIMENTAL METHODS

Chemical Reagents

Laponite® RD (Lap) was purchased from BYK company and was used without further modification. Grafting agent, 3-aminopropyltriethoxysilane (labeled as APTES) was supplied by Sigma-Aldrich Company assuming a purity grade up to 99%. General information about APTES are presented in Table S1. Strontium hexahydrated chloride ($SrCl_2 \cdot 6H_2O$, >99%) and Cobalt hexahydrated chloride ($CoCl_2 \cdot 6H_2O$, >98%) were supplied by Carl Roth company.

Chemical reagents and solvents such as HCl, NaOH, absolute ethanol, glycerol and phenoxypropanol, NaCl and $CaCl_2$ were supplied by Sigma-Aldrich company at analytical grade.

Synthesis of sylilated Laponites®

The protocol for the grafting of Lap can be detailed as follows. Six grams of Lap were mixed with 3.414 mL of APTES (i.e. 3.229 g) in a 200 mL solution of glycerol (Gly) or phenoxypropanol (Phe). After the addition of APTES, the solution was continuously stirred with a magnetic stirrer at 200 rpm during 24 hours, at 30, 60 or 90°C under Ar atmosphere.

The solid was then recovered by centrifugation at 8,000 rpm during 10 minutes before being rinsed two times with absolute ethanol and then two times with pure water (i.e. 2 g of adsorbent / 50 mL of solvent at each step) and being recovered between each rinse step by centrifugation at 8,000 rpm during 10 minutes. Then, the solid was dried in an oven at 60°C during 72 hours.

Silylated-Laps are hereafter labeled according to the synthesis solvent (i.e. Gly or Phe) and temperature (i.e. 30, 60 or 90°C) to be easily identified (e.g. Gly30, Phe60).

Experimental techniques

The experimental techniques allowing the fine characterization of Lap and Silylated-Laps (i.e. X-Ray Diffraction, Fourier transformed infra-red spectroscopy, Zeta potential, Thermogravimetric analyses and Nuclear Magnetic Resonance Spectroscopy) are detailed in Supplementary Information.

The concentrations of the different cations (Co^{2+} and Sr^{2+}) remaining in the adsorption of desorption solutions (water as solvent) were quantified with atomic absorption spectroscopy (AAS - Varian AA 240 FS), using the absorption mode and acetylene as fuel.

Adsorption experiments

Adsorption experiments were carried out both in single and mixed solutions both Sr^{2+} and Co^{2+} cations. Typically, the adsorbent mass was 100 mg in 100 mL of solution spiked with various concentrations of contaminant. The concentration of each contaminant ranged from 4.2 to 4,200 µM for Co^{2+} and 3.7 to 3,700 µM for Sr^{2+} in single-solute and from 4.2 to 2,100 µM for Co^{2+} and 3.7 to 1,350 µM for Sr^{2+} in mixed solutions (7 concentrations). The final solution was spiked at 0.1 mM of NaCl and let in interaction during 24 hours. This duration was previously determined on kinetic experiments (data not shown), in which the adsorption was completed after 5 minutes of interaction. The pH value of each solution was native and controlled at the beginning and at the end of interaction (i.e. pH values ranged between 6 and 6.5). Solutions were then centrifuged at 8,000 rpm during 10 minutes and the contaminant concentration in supernatant was analyzed by AAS.

Desorption experiments

After interaction with contaminants in the highest concentrated mixed experiment (i.e. the second highest concentration for single-solute experiment), adsorbents were

recovered by centrifugation at 8,000 rpm during 10 minutes. The recovered material was then dried at 60°C during 72 hours. 20 mg of dried adsorbent were then mixed with 20 mL of three different saline solutions; Pure water, 1 mM of $CaCl_2$ or 2 mM of NaCl. The solution was then gently stirred during one week at room temperature. Solutions were then centrifuged at 8,000 rpm during 10 minutes and the contaminant concentration in supernatant was analyzed by AAS.

Sorption modeling

The fit of the resulting adsorption isotherms by using Langmuir, Freundlich and Dubinin-Radushkevich (DR) equation models drives to numerous thermodynamic parameters allowing one to precisely quantify the affinity of contaminants with the sorbent. The model equations and parameters are detailed in Supporting Information.

RESULTS

Characterization of sylilated-Laponites® in various synthesis conditions

X-ray diffraction (XRD) patterns of Lap and silylated-Lap synthetized in various solvent and/or at different temperatures are presented in Figure 1. The XRD pattern of Lap displays broad reflections due to its low crystallinity and small particle size. The main

reflections at 7.0, 19.4, 34.2, and 61° 2Θ degrees are attributed to (001), (02,11), (13,20), and (060) reflections of the raw Lap, respectively.[35] Whatever the synthesis conditions, silylated-Laps display a shift to lower angular values of the reflection associated to (001) plane.[24] The shift extent varies both with the synthesis temperature and the solvent. The calculated basal spacings are 16.4, 14.5 and 14.5 Å at 30, 60 and 90°C respectively, for a synthesis in Gly and 15.4, 15.9 and 16.1 Å at 30, 60 and 90°C respectively for a synthesis in Phe. Globally, increasing the synthesis temperature in Gly leads to a decrease of the basal spacing of silylated-Laps while the adverse effect is observed in Phe. This evolution of the basal spacing could be related to the conformation of grafting agents (*i.e.* the formation of poly-siloxane multi-layers), or to the possible penetration of the interlayer space by APTES.[36,37]

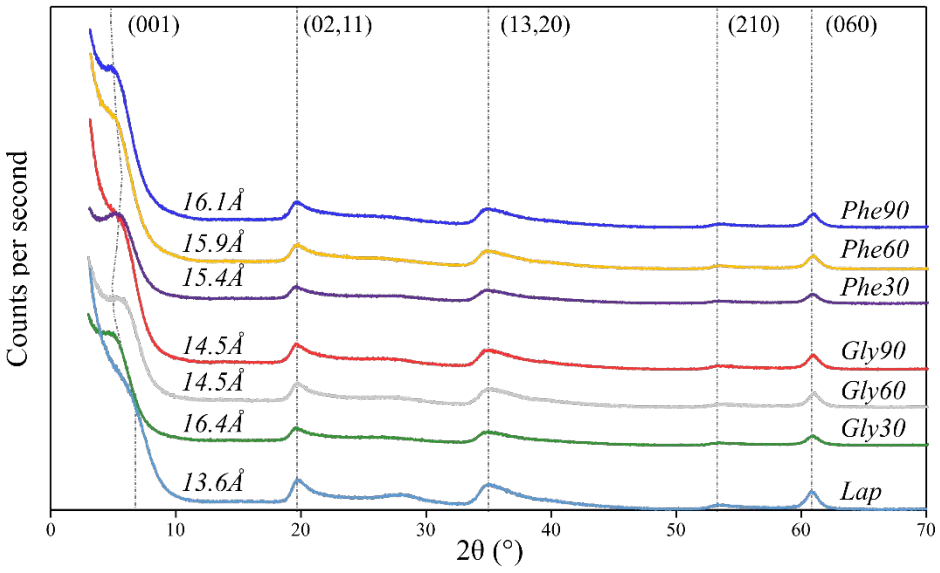

Figure 1. X-ray diffraction patterns of Lap and silylated-Laps for different synthesis solvents and temperatures.

Thermogravimetric (TG) analyses allow assessing the mass loss of the adsorbent during a gradual heating. Three main mass losses are expected during the heating of organo-modified clay minerals; (i) the evaporation of free and adsorbed water, below 150°C; (ii) the thermal oxidation of organic moieties (i.e. grafted/intercalated/adsorbed) between 150 and 600°C with a decomposition temperature depending on the characteristics of organic compounds[38] and; (iii) the dehydroxylation of clays beyond 600°C.[39,40]

The DTG curve of Lap (Figure 2) displays two main peaks at 55 and 720°C which correspond to the evaporation of adsorbed water and dehydroxylation of Lap respectively. DTG curves of silylated-Laps also present these two peaks, however, additional peaks appear at 265, 380 and 550°C, for all the samples, except Phe30. The presence of these peaks was already discussed in the literature and especially those at 265°C. Several assumptions assigned this mass loss to the decomposition of physisorbed APTES in the interlayer space,[33] or to the initial oxidation of aminopropyl moieties.[35,41] On the other hand, the mass losses around 380 and 550°C are attributed to the thermal oxidation of bonded APTES in the interlayer space and chemically grafted respectively.[38,42–44]

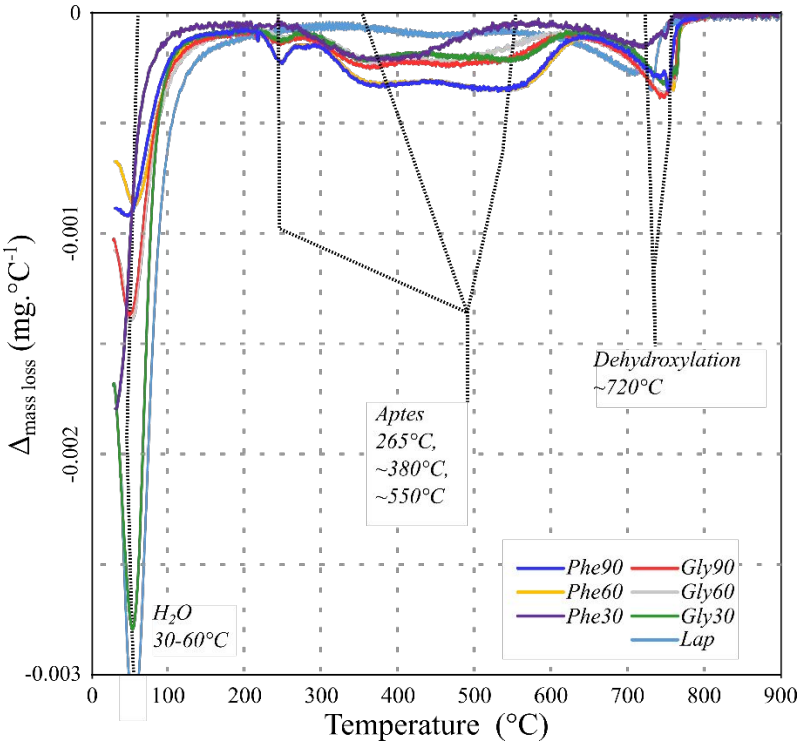

Figure 2. DTG curves of Lap and silylated-Laps for different synthesis solvents and temperatures.

The organic matter (OM) content of silylated-Laps can be derived from TG curves (Figure S1). These values allow to calculate the amount of adsorbed APTES that can be both compared to the initial load of APTES (i.e. resulted in the grafting yield) and to the exchange capacity of edge-sites of LAP (i.e. 0.36 mmol g^{-1}).[36] It is worthy to note that the OM content as well as the grafting yield increase with the synthesis temperature, even if this tendency is more pronounced for samples prepared in Phe. Indeed, the adsorbents

prepared in Gly exhibit an OM content of 3.5, 3.8 and 4.3 % when synthetized at 30, 60 and 90°C respectively, whereas for the solids synthetized in Phe, OM content of 1.5, 7.2 and 7.6 % are obtained at 30, 60 and 90°C respectively (Table S2). The highest grafting yield is obtained for Phe90 (i.e. 70.7 %) associated with an edge-sites occupation largely over 1 (i.e. 1.72). This saturation of edge-sites underlines the possibility of other interaction mechanisms than grafting. These samples also display the highest basal spacings, which may be related to the intercalation of APTES within the interlayer space of Lap.

Various bands are visible on the Fourier transformed infra-red (FTIR) spectrum of Lap at 1002, 693 and 662 cm^{-1}, and can be assigned to Si-O, Si-O-Si and Mg_3-OH respectively (Figure S2).[45] The spectrum of Lap also displays a small shoulder at 3680 cm^{-1}, assigned to surface hydroxyls groups. FTIR spectra of silylated-Laps show typical absorption bands of the organic compounds at 2880–2940 cm^{-1} relative to the symmetric and antisymmetric -CH_2 stretching vibrations of APTES, as well as the absorption bands between 1350 and 1600 cm^{-1} which are related to -CH_2 vibrations.[34,41] These specific bands testify the proper interaction between APTES and Lap. Some specific absorption bands are visible for the

samples synthetized in Phe, at 1250 and 2960 cm^{-1} respectively. The former is associated with C-O vibrations bands and the latter to $-CH_3$ vibration bands.[46] These two specific bands could be related to Phe itself or to APTES. An assumption can be made that either the grafting of APTES failed or was not complete either that Phe is associated with Lap.

Solid-state ^{1}H and ^{29} Si nuclear magnetic resonance (NMR) are powerful tools to gather information on the relative proportion of each type of protons as well as on the degree of condensation of APTES. As exhibited on the Lap ^{1}H magic angle spinning (MAS) solid state spectrum, three resonances are observed with chemical shifts equal to 4.5 ppm, 0.3 ppm and -0.5 ppm (Figure 3). The first one is assigned to adsorbed water molecules and the others are related to the structural –OH of LAP (*i.e.* -0.5 and 0.3 ppm).[47] After treatment with APTES, new resonances appear on the spectra of silylated-Laps prepared in Gly and in Phe (Figure 3). Thanks to the ACD/ ChemSketch 9.04 software, the assignment of each resonance due to APTES can be performed and is reported on the corresponding spectra according to the atom numbering of the organic group given in the inset of Figure 4. The presence of the protons assigned to aminopropyl group (labeled 4 and 5 in Figure 3) and related to triethoxy moieties (labeled 1 and 2 in Figure 3) is clearly

evidenced. A relative increase of the intensity of the resonances attributed to the protons from the aminopropyl moieties is observed for silylated-Laps prepared in Phe, especially between 30°C and higher temperatures, although the opposite pattern is displayed for sample prepared in Gly with a decrease between 30°C and higher temperatures (Figure 3).

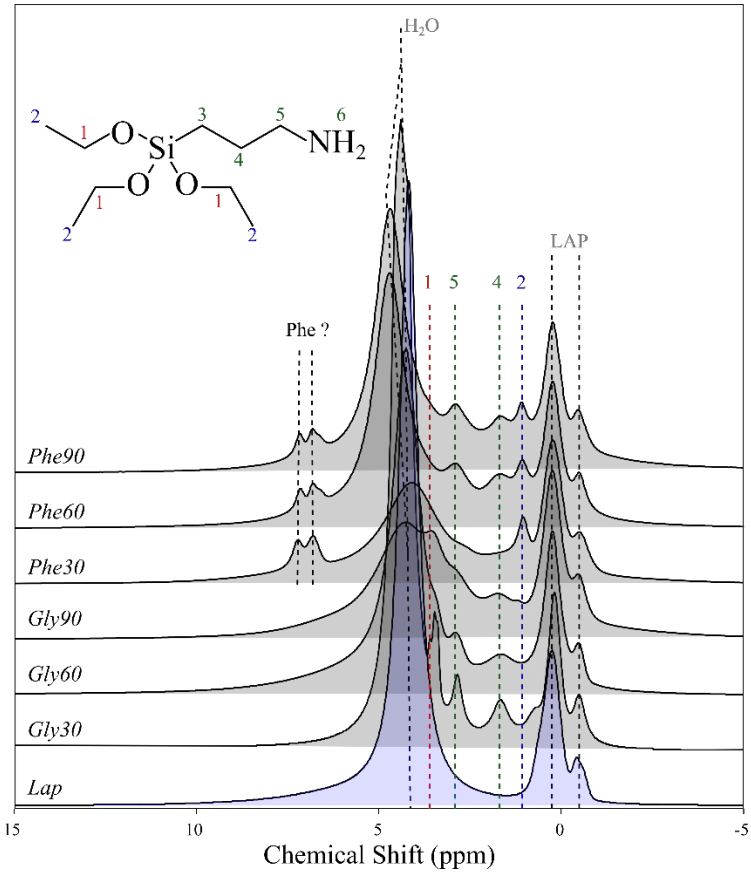

Figure 3. Solid-state ^{1}H NMR spectra of Lap and silylated-Laps for different synthesis solvents and temperatures.

It therefore confirms that increasing the temperature treatment does not lead to a significant increase of APTES content when Gly is used as solvent, whereas a significant increase is observed in Phe. In the same way, by increasing the synthesis temperature, the condensation of APTES is better performed in Phe, whereas non-significant impact is displayed in Gly. Finally, the ^{1}H NMR spectra of the silylated Lap in Phe also exhibit two specific resonances at 6.7 and 7.3 ppm. These signals can be assigned to C-H protons of Phe himself. This contribution of ^{1}H NMR spectra allows to confirm that the additional absorption bands observed in FTIR for the materials synthetized in Phe are generated by the association of Phe with the formed solids (Figure S2). This presence can be explained either by the washing process or by a specific interaction of Phe with silylated Lap, probably caused by its specific structure when compared to Gly.

Solid-state ^{29}Si NMR spectroscopy is a powerful tool to gather information on the different silicon species which are assigned based on conventional Q^n, T^n and M^n notations. Q, T and M are designated as tetra-, tri- and mono-functional units respectively, and *n* is the number of oxygen atoms further bonded to another silicon atom.[48] In the case of sylilated clay minerals, two types of silicon species are expected: Q^n species for the

silicon atoms belonging to structure (i.e. the tetrahedral sheet at the edges and from the silanol groups) and T^n species induced by the grafting of silane. These T^n species are usually written as following: $R\text{-}Si(OSi)_n(OH)_{n-3}$ where R stands for aminopropyl group in our case.

Two resonances at -95 and -85 ppm are displayed in the ^{29}Si NMR spectrum of Lap. The first one is attributed to Q^3 species within the tertrahedral sheets whereas the second one indicates the presence of Q^2 species, i.e. silanol groups at the edges of the Lap sheets or due to defects within the clay structure. It is worthy to note that the treatment with APTES leads to the decrease of the intensity of this latter resonance, indicating a decrease of the number of isolated edge-sites (Figure 4).[49] Concomitantly, two new resonances appear at -66 and -57 ppm, proving the grafting.[50]

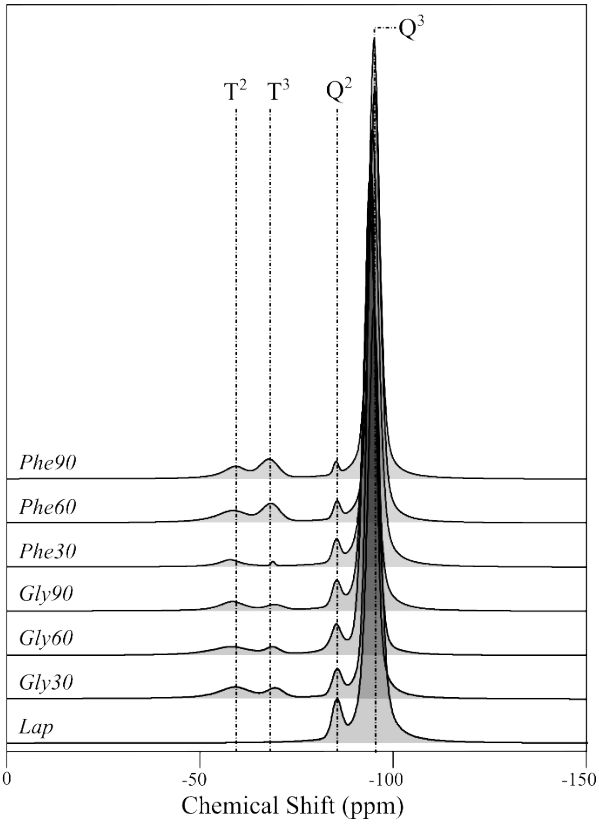

Figure 4. Solid state ^{29}Si NMR spectra of Lap and silylated-Laps for different synthesis solvents and temperatures.

The resonance at -66 ppm demonstrating the presence of T^3 (R $Si(OSi)_3$ units) and accompanying a reduction of the intensity of the resonance at -85 ppm confirms that a condensation reaction occurred between APTES and the silanol groups located at the edge and on the surface of the layers. On the other side, the resonance at -57 ppm is attributed to T^2 type environment, indicating a partial condensation of silicon species. The

T^3/T^2 ratio increases with the synthesis temperature in Phe although it remains unchanged whatever the temperature in Gly (Table S3). As well, the Q^3/Q^2 ratio also increases with the increase of the synthesis temperature in both Phe and Gly (Figure 4), indicating a lower number of silanol groups. This can be assigned to the grafting of APTES. The relative amount of Tn type species increases for the samples prepared in Phe as the temperature of the experiment is increased (especially between 30°C and higher synthesis temperatures), whereas the opposite pattern is observed in Gly. Hence, the grafting of APTES on edge-sites is favored in Phe whereas the interaction with surface sites is favored in Gly at 60 and 90°C.

Sorption Experiments

The single-solute adsorption isotherms of Sr^{2+} onto silylated-Laps are presented in Figure 5. The adsorption capacities range between 0.37 and 0.68 $mmol.g^{-1}$ for Phe30 and Phe60 respectively. Whatever the adsorbent, the adsorption isotherms exhibit a similar pattern with an increase of the adsorbed amount followed by a steady-state in the adsorption capacity for the highest starting concentrations.

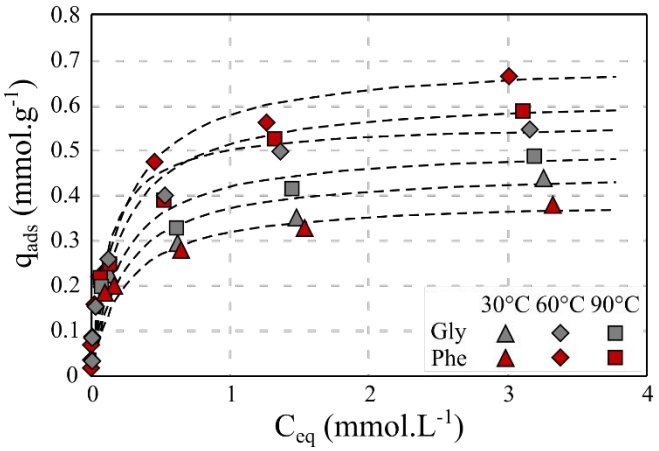

Figure 5. Single-solute adsorption isotherms of Sr^{2+} onto silylated-Laps synthetized in different conditions, dashed dark lines mark the Langmuir fits, with C_{eq} the equilibrium concentration and q_{ads} the adsorbed amount.

The adsorption isotherms of Sr^{2+} were properly fitted with the three used equations (Eq.1-Eq3, SI). Among them, the Langmuir equation produces the best fits with the experimental data (i.e. between 0.961 and 1.000, Table S4), allowing to assume that the adsorption may be limited to a monolayer. Both the solvent and the synthesis temperature impact the adsorption capacity of Sr^{2+}. Hence, the adsorbents synthetized at the lowest temperature display the lowest adsorption capacities (Figure 5). Conversely, the highest adsorption capacities among the three tested synthesis temperatures are noticed at 60°C (Table S4). This trend is confirmed whatever the synthesis solvent, even if the adsorption

capacities are higher for silylated-Laps synthetized in Phe than in Gly (i.e. if we except the lowest tested temperature).

The adsorption isotherms of Co^{2+} are gathered in Figure 6. As previously observed with Sr^{2+}, the adsorption isotherms display two distinct regimes with a strong increase of the adsorbed amount followed by a steady state for the highest starting concentration. However, the adsorption of Co^{2+} appears to be more favorable than that of Sr^{2+}, with insignificant equilibrium concentrations in a wider range of starting concentrations (Figure 6).

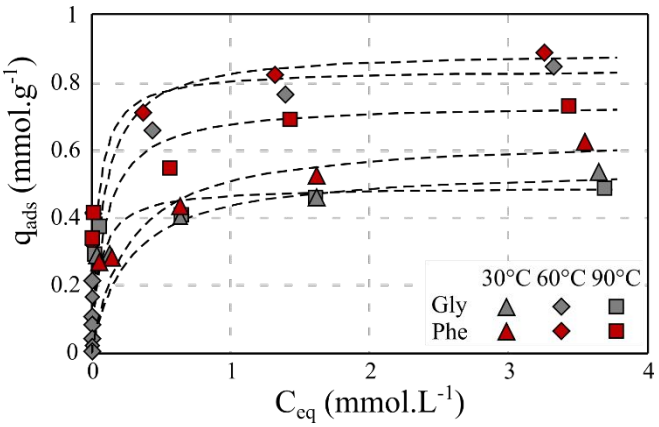

Figure 6. Single-solute adsorption isotherms of Co^{2+} onto silylated-Laps synthetized in different conditions, dashed dark lines marks the Langmuir fits, with C_{eq} the equilibrium concentration and q_{ads} the adsorbed amount.

The adsorption capacities ranged from 0.48 and 0.89 mmol.g^{-1} for Gly90 and Phe60 respectively. The adsorption isotherms are properly fitted by the Langmuir model, except for the two adsorbents synthetized at 30°C, for which the Freundlich equation displays better fits with experimental data. These two latter isotherms exhibit the lowest K_L values among the tested adsorbents, indicating a lower affinity with Co^{2+} (Table S4). It can be concluded that the synthesis temperature strongly influences the affinity between Co^{2+} and silylated-Laps, and as observed before with Sr^{2+}, the highest adsorption capacities are noticed at 60°C. The solvent appears to be less significant in the adsorbed amount of Co^{2+}, except at 90°C, for which the adsorption capacity is significantly higher for the silylated-Lap prepared in Phe than in Gly.

Bi-solute experiments were conducted in the same conditions and the adsorption isotherms are presented in Figure S3 and S4. The competition between Sr^{2+} and Co^{2+} impacts the adsorption capacities in the same extent whatever the adsorbent. It is worthy to note that the adsorption capacities of Co^{2+} are moderately affected with a decrease around 25% although the adsorption capacities of Sr^{2+} decrease in a more significant extent around 40% (Figure S3 and S4). In parallel to these modifications, no significant

variation is observed on the thermodynamic constants, indicating similar interaction mechanisms in single and bi-solute experiments (Table S4).

Desorption Experiments

The desorption experiments were conducted in three different solutions (i.e. pure water, 2 mM NaCl and 1 mM $CaCl_2$) with silylated-Laps prepared in various conditions. The desorption yields of Sr^{2+} and Co^{2+} are presented in Figure 7 and 8, respectively. The desorption yields of Sr^{2+} (i.e. between 1 and 32 %) are higher than that of Co^{2+} (i.e. between 0.1 and 4.2 %). Moreover, the desorption yield of Sr^{2+} generally increases for the same sample from pure water to the solution containing 1 mM $CaCl_2$ (Figure 7). Hence, the presence of an inorganic cation with the same valence as Sr^{2+} increases its desorption. The same pattern is visible on the desorbed amount of Co^{2+}, even if the whole desorption remains lower than that of Sr^{2+}.

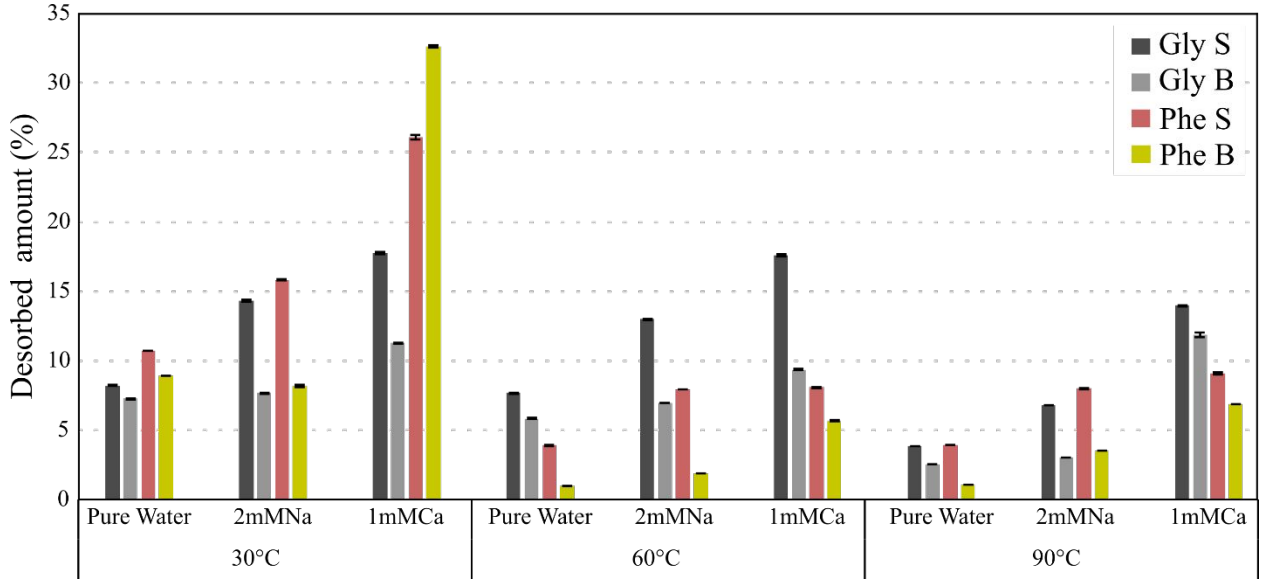

Figure 7. Desorption yield of Sr^{2+} as a function of the synthesis temperature of the adsorbent and the releasing solution with samples labeled according to the synthesis solvent (Gly or Phe) and the type of adsorption experiment (S for single-solute and B for bi-solute).

The composition of the solution during the adsorption experiment also impacts the desorption yield. Hence, the desorbed amount is systematically lower when both Sr^{2+} and Co^{2+} were previously adsorbed than in single-solute experiment. This result can be understood through the equilibrium processes between solid and liquid phase that would happen in a different extent in two cations were previously adsorbed.[51]

For a same releasing solution, the desorption yield of Sr^{2+} is systematically higher in Gly in comparison with Phe at 60°C and 90°C (Figure 7). Concerning Co^{2+} desorption, the opposite pattern is observed (except for synthesis performed at 90°C, Figure 8). This result suggests that the conformation of the grafting agent, which is different after synthesis in Phe or Gly also impacts the adsorption mechanisms of Sr^{2+} and Co^{2+} onto the adsorbents. Hence, the stronger release of Co^{2+} from silylated-Laps synthetized in Phe could suggest that a significant part of this cation is adsorbed through cation exchange (i.e. more sensible to the presence of Ca^{2+}). However, this pattern is obvious at 30 and 60 °C but is not consistent at 90°C. The modification of the synthesis temperature therefore involves such complex reaction mechanisms that could be not linear. In this way, the desorbed amount of Co^{2+} are the lowest for the adsorbents synthetized at 90°C.

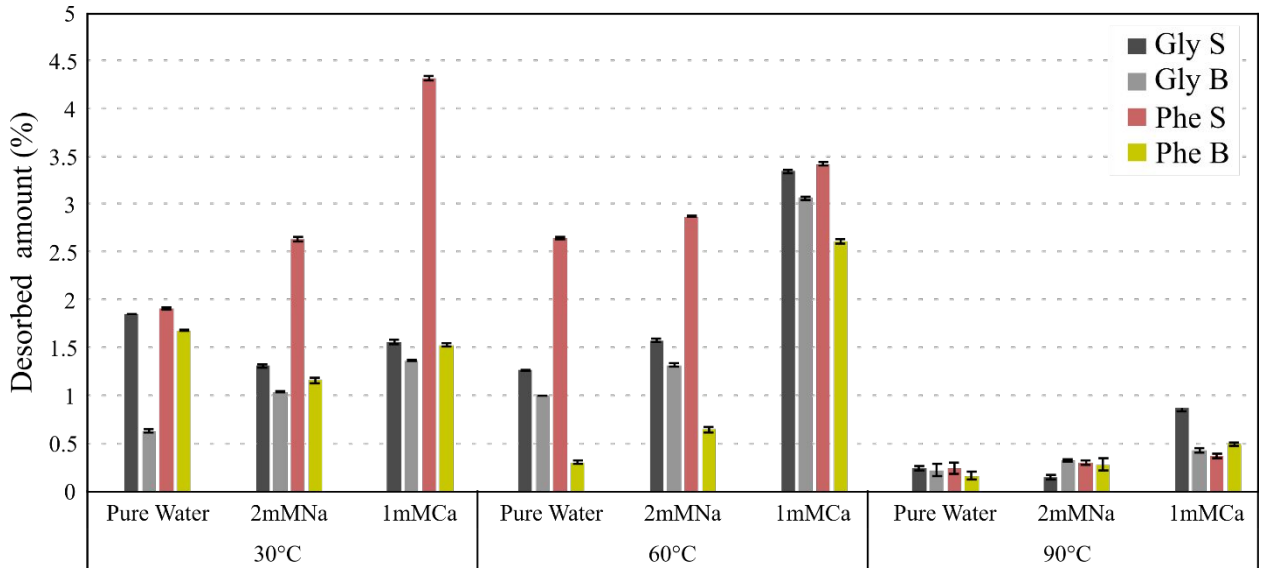

Figure 8. Desorption yield of Co^{2+} as a function of the synthesis temperature of the adsorbent and the releasing solution.

From these results, it can be concluded that the adsorption of Co^{2+} onto the synthetized adsorbents is very stable with low desorbed amounts whatever the releasing solutions. Globally, the increase of the synthesis temperature decreases the desorption yield of Co^{2+}, except in 1mM $CaCl_2$ solution, in which ion exchange may occur. In the same way, the desorption yield of Sr^{2+} is impacted by the synthesis temperature (i.e. decreasing with increasing temperature) and by the composition of the solution, as the desorption yield is the highest in 1 mM $CaCl_2$ solution.

DISCUSSION

Impact of the synthesis conditions on the resulted hybrid materials

The effects of the solvent and of the temperature on the synthesis of silylated-Laps were tested, and both of them significantly impacted the structure of the resulting solids.

According to the literature, the two main characteristics of a solvent that may impact the grafting reaction are the polarity and the surface energy.[52,53] In this work, Phe and Gly were used, with a surface energy of 37.7 and 63.4 $mN.m^{-1}$, respectively. It is therefore expected that the interaction between APTES and Lap could be preferentially realized through intercalation for a synthesis in Gly than in Phe.[44] This assumption is partially validated by the results, in which the mass losses associated to the intercalation of APTES were higher in Gly than in Phe. However, the whole grafting reaction results in higher organic matter content for hybrids prepared in Phe. This can be explained by the presence of a significant amount of Phe (Figure 4) within silylated-Laps, despite flushing, that increased the organic matter content without any improvement of the grafting reaction. Yet, the grafting reaction was better performed in Phe than in Gly, as revealed by the ^{29}Si NMR spectroscopy analysis (Figure 4). For the two highest tested temperatures, the Q^3/Q^2 ratio was higher in Phe than in Gly, indicating a better grafting

on the edge-sites of Lap. Consistently, the grafting onto surface sites was also higher in Phe than in Gly, exhibiting by the value of $\sum T$ (Table S3).

In parallel to the effect of the dispersing media, the impact of the temperature was also evaluated. The organic matter content increased with the temperature in both Phe and Gly (Table S2). This increase was more important in the former, although the lowest organic matter content was noticed for Phe30 with 1.5 %. This sample was also the only which did not display any characteristic mass losses of APTES (Figure 2). Beyond the influence of the amount of grafted APTES, the increase of the temperature of the treatment also affected the whole structure of the silylated Lap. The increase of the basal spacings with the temperature in Phe was opposed to its decrease in Gly. As a result, it can be concluded that the favorable intercalation in Gly at low temperature (*i.e.* higher basal spacing, Figure 1) is balanced by a better achievement of the grafting reaction at higher temperature. Conversely, in Phe, the intercalation was not favored explaining the low organic content at 30°C, although the grafting reaction was enhanced for the highest temperatures.[34,54]

Impact of the synthesis conditions on the sorption mechanisms of ions onto hybrid materials

According to the results, the adsorption capacities of Co^{2+} and Sr^{2+} were systematically higher than the CEC of Lap (i.e. 75 meq.100g^{-1}).[55] Cation exchange was therefore a potential sorption mechanism of both Co^{2+} and Sr^{2+} but can't be the sole. The lowest adsorption capacity of Sr^{2+} is displayed by Phe30 with 0.36 mmol.g^{-1}, and therefore close to the CEC of Lap. Yet, this adsorbent displayed the lowest grafted APTES amount, emphasizing the possible adsorption of Sr^{2+} through cation exchange on this sample (Figure 6). The increase of the APTES content on varying the synthesis conditions was strongly correlated with the adsorption capacity of Sr^{2+} (Figure S5). The higher the APTES content, the higher the adsorption capacity of Sr^{2+}, indicating possible binding mechanisms with grafted organic moieties.[56] The only limitation on this correlation was the higher adsorption capacity of Sr^{2+} for the treatment carried out at 60°C than at 90°C. This can be explained by a potential locking effect for the highest contents of APTES, limiting the availability of adsorption sites for Sr^{2+}.[57] This assumption was especially highlighted by the lower desorption yield of Sr^{2+} for the silylated-Laps synthetized at

higher temperatures, indicating that the lower availability of adsorption sites during adsorption experiments similarly impacted the desorption.

The adsorption capacities of Co^{2+} are more difficult to understand. No significant correlation can be indeed established with parameters such as the APTES content (Figure S5). The two lowest adsorption capacities were noticed onto Gly30 and Gly90. Due to the preferential intercalation of APTES rather than grafting onto the edge-sites in this solvent, it can be assumed that the locking effect of the interlayer hinders in a significant extent the availability of the adsorption sites of Co^{2+} in this solvent. Reversely, for the silylated clay minerals synthetized in Phe, the highest adsorption capacity was noticed for a synthesis at 60°C and the lowest at 30°C, like previously observed for Sr^{2+}. The prime grafting onto the edge-sites in this solvent would explain the higher adsorption capacity of Co^{2+}, which could be both adsorbed through cation exchange and binding with APTES moieties.[4,7,58] Due to its very weak desorption whatever the releasing solutions, the latter mechanism is favored, especially for silylated-Laps synthetized at 90°C (Figure 8).

CONCLUSIONS

In this study, silylated Laponites® were successfully prepared under various conditions. The influence of the solvent and temperature during synthesis were assessed. From the results, increasing the synthesis temperature appeared to be favorable in maximizing the APTES content, whereas the solvent played a key role in the extent and location of grafting reaction. Yet, the highest adsorption capacity of Sr^{2+} and Co^{2+} was not systematically correlated with the highest APTES content. Sr^{2+} was mostly adsorbed through cation exchange although the main adsorption mechanism of Co^{2+} was the strong electrostatic interaction with APTES moieties. The competition between the two adsorbates resulted in a better selectivity for adsorption for Co^{2+} in comparison with Sr^{2+}. This better selectivity for adsorption was demonstrated during releasing experiments, in which the desorption of Co^{2+} was very weak, especially when the treatment was carried out at 90°C. Finally, glycerol may be preferred due to its miscibility with water, reversely instead of phenoxypropanol, which needs ethanol to be properly rinsed.

Even if further tests need to be conducted to validate the potential of such adsorbent for the removal of radionuclides within real radioactive wastes, the presented results could pave the way for the use of green solvents in order to synthetize efficient adsorbents for

the removal of radionuclides from aqueous wastes, and this approach was patented.[59] Simultaneously, this work provides new insights on the impact of synthesis temperature on the silylation of clay minerals. Notably, even if the increase of the synthesis temperature increases silane content, this parameter did not systematically result in an enhancement of the adsorption capacity.

SUPPORTING INFORMATION. The supporting include a description of the experimental techniques used for the characterization of materials, a deeper description of the used equations for the modeling of the adsorption isotherms, Table S1 displays the physico-chemical properties of APTES, Table S2 shows the calculations derived from TG curves, Table S3 shows the ratios derived from ^{29}Si NMR spectra, Table S4 displays the thermodynamic parameters derived from adsorption modeling, Figure S1 displays the TG curves of the materials, Figure S2 displays the FTIR spectra of the adsorbents, Figure S3-S4 display the bi-solute adsorption isotherms of Co^{2+} and Sr^{2+} onto the adsorbents and Figure S5 displays the relationship between adsorbed amount of Co^{2+} and Sr^{2+} and the APTES content of the materials. The following files are

available free of charge.

ACKNOWLEDGMENT

L. Michelin and S. Rigolet are gratefully thanked for their technical support. The ONET Technologies company is acknowledged for funding this study.

REFERENCES

(1) Claverie, M.; Garcia, J.; Prevost, T.; Brendlé, J.; Limousy, L. Inorganic and Hybrid (Organic–Inorganic) Lamellar Materials for Heavy Metals and Radionuclides Capture in Energy Wastes Management—A Review. *Materials* **2019**, *12* (9), 1399. https://doi.org/10.3390/ma12091399.

(2) Ma, B.; Oh, S.; Shin, W. S.; Choi, S.-J. Removal of Co2+, Sr2+ and Cs+ from Aqueous Solution by Phosphate-Modified Montmorillonite (PMM). *Desalination* **2011**, *276* (1), 336–346. https://doi.org/10.1016/j.desal.2011.03.072.

(3) Moyo, F.; Tandlich, R.; Wilhelmi, B. S.; Balaz, S. Sorption of Hydrophobic Organic Compounds on Natural Sorbents and Organoclays from Aqueous and Non-Aqueous Solutions: A Mini-Review. *International Journal of Environmental Research and Public Health* **2014**, *11* (5), 5020–5048. https://doi.org/10.3390/ijerph110505020.

(4) Thiebault, T.; Brendlé, J.; Augé, G.; Limousy, L. Zwitterionic-Surfactant Modified LAPONITE®s for Removal of Ions (Cs+, Sr2+ and Co2+) from Aqueous Solutions as a Sustainable Recovery Method for Radionuclides from Aqueous Wastes. *Green Chem.* **2019**, *21* (18), 5118–5127. https://doi.org/10.1039/C9GC02243K.

(5) Uddin, M. K. A Review on the Adsorption of Heavy Metals by Clay Minerals, with Special Focus on the Past Decade. *Chemical Engineering Journal* **2017**, *308*, 438–462. https://doi.org/10.1016/j.cej.2016.09.029.

(6) de Oliveira, T.; Guégan, R.; Thiebault, T.; Milbeau, C. L.; Muller, F.; Teixeira, V.; Giovanela, M.; Boussafir, M. Adsorption of Diclofenac onto Organoclays: Effects of Surfactant and Environmental (PH and Temperature) Conditions. *Journal of Hazardous Materials* **2017**, *323*, *Part A*, 558–566. https://doi.org/10.1016/j.jhazmat.2016.05.001.

(7) Kara, M.; Yuzer, H.; Sabah, E.; Celik, M. S. Adsorption of Cobalt from Aqueous Solutions onto Sepiolite. *Water Research* **2003**, *37* (1), 224–232. https://doi.org/10.1016/S0043-1354(02)00265-8.

(8) Thiebault, T. Raw and Modified Clays and Clay Minerals for the Removal of Pharmaceutical Products from Aqueous Solutions: State of the Art and Future Perspectives. *Critical Reviews in Environmental Science and Technology* **2019**. https://doi.org/10.1080/10643389.2019.1663065.

(9) de Paiva, L. B.; Morales, A. R.; Valenzuela Díaz, F. R. Organoclays: Properties, Preparation and Applications. *Applied Clay Science* **2008**, *42* (1–2), 8–24. https://doi.org/10.1016/j.clay.2008.02.006.

(10) Guégan, R. Organoclay Applications and Limits in the Environment. *Comptes Rendus Chimie* **2019**, *22* (2–3), 132–141. https://doi.org/10.1016/j.crci.2018.09.004.

(11) Park, Y.; Ayoko, G. A.; Frost, R. L. Application of Organoclays for the Adsorption of Recalcitrant Organic Molecules from Aqueous Media. *Journal of Colloid and Interface Science* **2011**, *354* (1), 292–305. https://doi.org/10.1016/j.jcis.2010.09.068.

(12) Xu, S.; Sheng, G.; Boyd, S. A. Use of Organoclays in Pollution Abatement. *Advances in Agronomy* **1997**, *59*, 25–62. https://doi.org/10.1016/S0065-2113(08)60052-8.

(13) de Mello Ferreira Guimarães, A.; Ciminelli, V. S. T.; Vasconcelos, W. L. Smectite Organofunctionalized with Thiol Groups for Adsorption of Heavy Metal Ions. *Applied Clay Science* **2009**, *42* (3), 410–414. https://doi.org/10.1016/j.clay.2008.04.006.

(14) Guerra, D. L.; Oliveira, S. P.; Silva, R. A. S.; Silva, E. M.; Batista, A. C. Dielectric Properties of Organofunctionalized Kaolinite Clay and Application in Adsorption

Mercury Cation. *Ceramics International* **2012**, *38* (2), 1687–1696. https://doi.org/10.1016/j.ceramint.2011.09.062.

(15) He, H.; Ma, L.; Zhu, J.; Frost, R. L.; Theng, B. K. G.; Bergaya, F. Synthesis of Organoclays: A Critical Review and Some Unresolved Issues. *Applied Clay Science* **2014**, *100*, 22–28. https://doi.org/10.1016/j.clay.2014.02.008.

(16) Struijk, M.; Rocha, F.; Detellier, C. Novel Thio-Kaolinite Nanohybrid Materials and Their Application as Heavy Metal Adsorbents in Wastewater. *Applied Clay Science* **2017**, *150*, 192–201. https://doi.org/10.1016/j.clay.2017.09.024.

(17) Wamba, A. G. N.; Kofa, G. P.; Koungou, S. N.; Thue, P. S.; Lima, E. C.; dos Reis, G. S.; Kayem, J. G. Grafting of Amine Functional Group on Silicate Based Material as Adsorbent for Water Purification: A Short Review. *Journal of Environmental Chemical Engineering* **2018**, *6* (2), 3192–3203. https://doi.org/10.1016/j.jece.2018.04.062.

(18) Zhang, Z. Z.; Sparks, D. L.; Scrivner, N. C. Sorption and Desorption of Quaternary Amine Cations on Clays. *Environmental science & technology* **1993**, *27* (8), 1625–1631.

(19) He, H.; Zhou, Q.; Martens, W. N.; Kloprogge, T. J.; Yuan, P.; Xi, Y.; Zhu, J.; Frost, R. L. Microstructure of HDTMA+-Modified Montmorillonite and Its Influence on Sorption Characteristics. *Clays and Clay Minerals* **2006**, *54* (6), 689–696. https://doi.org/info:doi/10.1346/CCMN.2006.0540604.

(20) Awad, A. M.; Shaikh, S. M. R.; Jalab, R.; Gulied, M. H.; Nasser, M. S.; Benamor, A.; Adham, S. Adsorption of Organic Pollutants by Natural and Modified Clays: A Comprehensive Review. *Separation and Purification Technology* **2019**, *228*, 115719. https://doi.org/10.1016/j.seppur.2019.115719.

(21) Buruga, K.; Song, H.; Shang, J.; Bolan, N.; Jagannathan, T. K.; Kim, K.-H. A Review on Functional Polymer-Clay Based Nanocomposite Membranes for Treatment of Water. *Journal of Hazardous Materials* **2019**, *379*, 120584. https://doi.org/10.1016/j.jhazmat.2019.04.067.

(22) Jaber, M.; Miehé-Brendlé, J.; Michelin, L.; Delmotte, L. Heavy Metal Retention by Organoclays: Synthesis, Applications, and Retention Mechanism. *Chem. Mater.* **2005**, *17* (21), 5275–5281. https://doi.org/10.1021/cm050754i.

(23) Kostenko, L. S.; Tomashchuk, I. I.; Kovalchuk, T. V.; Zaporozhets, O. A. Bentonites with Grafted Aminogroups: Synthesis, Protolytic Properties and Assessing Cu(II), Cd(II) and Pb(II) Adsorption Capacity. *Applied Clay Science* **2019**, *172*, 49–56. https://doi.org/10.1016/j.clay.2019.02.009.

(24) Mercier, L.; Pinnavaia, T. J. A Functionalized Porous Clay Heterostructure for Heavy Metal Ion (Hg2+) Trapping. *Microporous and Mesoporous Materials* **1998**, *20* (1), 101–106. https://doi.org/10.1016/S1387-1811(97)00019-X.

(25) Gershey, E. L.; Klein, R. C.; Party, E.; Wilkerson, A. *Low-Level Radioactive Waste*; Van Nostrand Reinhold Co.: New York, NY, 1990.

(26) Salbu, B.; Lind, O. C.; Skipperud, L. Radionuclide Speciation and Its Relevance in Environmental Impact Assessments. *Journal of Environmental Radioactivity* **2004**, *74* (1), 233–242. https://doi.org/10.1016/j.jenvrad.2004.01.008.

(27) Periáñez, R.; Bezhenar, R.; Brovchenko, I.; Duffa, C.; Iosjpe, M.; Jung, K. T.; Kobayashi, T.; Lamego, F.; Maderich, V.; Min, B. I.; et al. Modelling of Marine Radionuclide Dispersion in IAEA MODARIA Program: Lessons Learnt from the Baltic Sea and Fukushima Scenarios. *Science of The Total Environment* **2016**, *569–570*, 594–602. https://doi.org/10.1016/j.scitotenv.2016.06.131.

(28) Rosenberg, B. L.; Ball, J. E.; Shozugawa, K.; Korschinek, G.; Hori, M.; Nanba, K.; Johnson, T. E.; Brandl, A.; Steinhauser, G. Radionuclide Pollution inside the Fukushima Daiichi Exclusion Zone, Part 1: Depth Profiles of Radiocesium and Strontium-90 in Soil. *Applied Geochemistry* **2017**, *85*, 201–208. https://doi.org/10.1016/j.apgeochem.2017.06.003.

(29) de Gisi, S.; Lofrano, G.; Grassi, M.; Notarnicola, M. Characteristics and Adsorption Capacities of Low-Cost Sorbents for Wastewater Treatment: A Review. *Sustainable Materials and Technologies* **2016**, *9*, 10–40. https://doi.org/10.1016/j.susmat.2016.06.002.

(30) Tran, H. N.; Nguyen, H. C.; Woo, S. H.; Nguyen, T. V.; Vigneswaran, S.; Hosseini-Bandegharaei, A.; Rinklebe, J.; Sarmah, A. K.; Ivanets, A.; Dotto, G. L.; et al. Removal of Various Contaminants from Water by Renewable Lignocellulose-Derived Biosorbents: A Comprehensive and Critical Review. *Critical Reviews in*

Environmental Science and Technology **2019**, *0* (0), 1–65. https://doi.org/10.1080/10643389.2019.1607442.

(31) Jessop, P. G. Searching for Green Solvents. *Green Chemistry* **2011**, *13* (6), 1391–1398. https://doi.org/10.1039/C0GC00797H.

(32) Gu, Y.; Jérôme, F. Glycerol as a Sustainable Solvent for Green Chemistry. *Green Chemistry* **2010**, *12* (7), 1127–1138. https://doi.org/10.1039/C001628D.

(33) Yang, S.; Yuan, P.; He, H.; Qin, Z.; Zhou, Q.; Zhu, J.; Liu, D. Effect of Reaction Temperature on Grafting of γ-Aminopropyl Triethoxysilane (APTES) onto Kaolinite. *Applied Clay Science* **2012**, *62–63*, 8–14. https://doi.org/10.1016/j.clay.2012.04.006.

(34) He, H.; Tao, Q.; Zhu, J.; Yuan, P.; Shen, W.; Yang, S. Silylation of Clay Mineral Surfaces. *Applied Clay Science* **2013**, *71*, 15–20. https://doi.org/10.1016/j.clay.2012.09.028.

(35) Park, M.; Shim, I.-K.; Jung, E.-Y.; Choy, J.-H. Modification of External Surface of Laponite by Silane Grafting. *Journal of Physics and Chemistry of Solids* **2004**, *65* (2), 499–501. https://doi.org/10.1016/j.jpcs.2003.10.031.

(36) Negrete Herrera, N.; Letoffe, J.-M.; Reymond, J.-P.; Bourgeat-Lami, E. Silylation of Laponite Clay Particles with Monofunctional and Trifunctional Vinyl Alkoxysilanes. *Journal of Materials Chemistry* **2005**, *15* (8), 863–871. https://doi.org/10.1039/B415618H.

(37) Tao, Q.; Fang, Y.; Li, T.; Zhang, D.; Chen, M.; Ji, S.; He, H.; Komarneni, S.; Zhang, H.; Dong, Y.; et al. Silylation of Saponite with 3-Aminopropyltriethoxysilane. *Applied Clay Science* **2016**, *132–133*, 133–139. https://doi.org/10.1016/j.clay.2016.05.026.

(38) Asgari, M.; Sundararaj, U. Silane Functionalization of Sodium Montmorillonite Nanoclay: The Effect of Dispersing Media on Intercalation and Chemical Grafting. *Applied Clay Science* **2018**, *153*, 228–238. https://doi.org/10.1016/j.clay.2017.12.020.

(39) Emmerich, K.; Madsen, F. T.; Kahr, G. Dehydroxylation Behavior of Heat-Treated and Steam-Treated Homoionic Cis-Vacant Montmorillonites. *Clays Clay Miner.* **1999**, *47* (5), 591–604. https://doi.org/10.1346/CCMN.1999.0470506.

(40) Xie, W.; Gao, Z.; Liu, K.; Pan, W.-P.; Vaia, R.; Hunter, D.; Singh, A. Thermal Characterization of Organically Modified Montmorillonite. *Thermochimica Acta* **2001**, *367–368*, 339–350. https://doi.org/10.1016/S0040-6031(00)00690-0.

(41) Avila, L. R.; de Faria, E. H.; Ciuffi, K. J.; Nassar, E. J.; Calefi, P. S.; Vicente, M. A.; Trujillano, R. New Synthesis Strategies for Effective Functionalization of Kaolinite and Saponite with Silylating Agents. *Journal of Colloid and Interface Science* **2010**, *341* (1), 186–193. https://doi.org/10.1016/j.jcis.2009.08.041.

(42) Fenero, M.; Palenzuela, J.; Azpitarte, I.; Knez, M.; Rodríguez, J.; Tena-Zaera, R. Laponite-Based Surfaces with Holistic Self-Cleaning Functionality by Combining Antistatics and Omniphobicity. *ACS Appl. Mater. Interfaces* **2017**, *9* (44), 39078–39085. https://doi.org/10.1021/acsami.7b13535.

(43) Parolo, M. E.; Pettinari, G. R.; Musso, T. B.; Sánchez-Izquierdo, M. P.; Fernández, L. G. Characterization of Organo-Modified Bentonite Sorbents: The Effect of Modification Conditions on Adsorption Performance. *Applied Surface Science* **2014**, *320*, 356–363. https://doi.org/10.1016/j.apsusc.2014.09.105.

(44) Shanmugharaj, A. M.; Rhee, K. Y.; Ryu, S. H. Influence of Dispersing Medium on Grafting of Aminopropyltriethoxysilane in Swelling Clay Materials. *Journal of Colloid and Interface Science* **2006**, *298* (2), 854–859. https://doi.org/10.1016/j.jcis.2005.12.049.

(45) Pálková, H.; Madejová, J.; Zimowska, M.; Serwicka, E. M. Laponite-Derived Porous Clay Heterostructures: II. FTIR Study of the Structure Evolution. *Microporous and Mesoporous Materials* **2010**, *127* (3), 237–244. https://doi.org/10.1016/j.micromeso.2009.07.012.

(46) DesLauriers, P. J.; Rohlfing, D. C.; Hsieh, E. T. Quantifying Short Chain Branching Microstructures in Ethylene 1-Olefin Copolymers Using Size Exclusion Chromatography and Fourier Transform Infrared Spectroscopy (SEC–FTIR). *Polymer* **2002**, *43* (1), 159–170. https://doi.org/10.1016/S0032-3861(01)00574-2.

(47) Alba, M. D.; Becerro, A. I.; Castro, M. A.; Perdigón, A. C. High-Resolution 1H MAS NMR Spectra of 2:1 Phyllosilicates. *Chemical Communications* **2000**, *0* (1), 37–38. https://doi.org/10.1039/A906577F.

(48) Brendlé, J. Organic–Inorganic Hybrids Having a Talc-like Structure as Suitable Hosts to Guest a Wide Range of Species. *Dalton Transactions* **2018**, *47* (9), 2925–2932. https://doi.org/10.1039/C7DT03902F.

(49) Borsacchi, S.; Geppi, M.; Ricci, L.; Ruggeri, G.; Veracini, C. A. Interactions at the Surface of Organophilic-Modified Laponites: A Multinuclear Solid-State NMR Study. *Langmuir* **2007**, *23* (7), 3953–3960. https://doi.org/10.1021/la063040a.

(50) Negrete Herrera, N.; Letoffe, J.-M.; Putaux, J.-L.; David, L.; Bourgeat-Lami, E. Aqueous Dispersions of Silane-Functionalized Laponite Clay Platelets. A First Step toward the Elaboration of Water-Based Polymer/Clay Nanocomposites. *Langmuir* **2004**, *20* (5), 1564–1571. https://doi.org/10.1021/la0349267.

(51) Arias, M.; Pérez-Novo, C.; López, E.; Soto, B. Competitive Adsorption and Desorption of Copper and Zinc in Acid Soils. *Geoderma* **2006**, *133* (3), 151–159. https://doi.org/10.1016/j.geoderma.2005.07.002.

(52) Asgari, M.; Sundararaj, U. Pre-Exfoliated Nanoclay through Two Consecutive Reaction Systems: Silane Functionalization Followed by Grafting of Amino Acid Monomers. *Applied Clay Science* **2018**, *151*, 81–91. https://doi.org/10.1016/j.clay.2017.10.021.

(53) Su, L.; Tao, Q.; He, H.; Zhu, J.; Yuan, P.; Zhu, R. Silylation of Montmorillonite Surfaces: Dependence on Solvent Nature. *Journal of Colloid and Interface Science* **2013**, *391*, 16–20. https://doi.org/10.1016/j.jcis.2012.08.077.

(54) Piscitelli, F.; Posocco, P.; Toth, R.; Fermeglia, M.; Pricl, S.; Mensitieri, G.; Lavorgna, M. Sodium Montmorillonite Silylation: Unexpected Effect of the Aminosilane Chain Length. *Journal of Colloid and Interface Science* **2010**, *351* (1), 108–115. https://doi.org/10.1016/j.jcis.2010.07.059.

(55) Negrete-Herrera, N.; Putaux, J.-L.; Bourgeat-Lami, E. Synthesis of Polymer/Laponite Nanocomposite Latex Particles via Emulsion Polymerization Using Silylated and Cation-Exchanged Laponite Clay Platelets. *Progress in Solid State Chemistry* **2006**, *34* (2), 121–137. https://doi.org/10.1016/j.progsolidstchem.2005.11.040.

(56) Liu, C.; Liu, S.; Wu, P.; Dai, Y.; Tran, L.; Zhu, N.; Guo, C.; Sohoo, I. Enhancing the Adsorption Behavior and Mechanism of Sr(II) by Functionalized Montmorillonite

with Different 3-Aminopropyltriethoxysilane (APTES) Ratios. *RSC Adv.* **2016**, *6* (86), 83288–83295. https://doi.org/10.1039/C6RA19362E.

(57) Su, L.; Tao, Q.; He, H.; Zhu, J.; Yuan, P. Locking Effect: A Novel Insight in the Silylation of Montmorillonite Surfaces. *Materials Chemistry and Physics* **2012**, *136* (2), 292–295. https://doi.org/10.1016/j.matchemphys.2012.07.010.

(58) Liang, X.; Xu, Y.; Tan, X.; Wang, L.; Sun, Y.; Lin, D.; Sun, Y.; Qin, X.; Wang, Q. Heavy Metal Adsorbents Mercapto and Amino Functionalized Palygorskite: Preparation and Characterization. *Colloids and Surfaces A: Physicochemical and Engineering Aspects* **2013**, *426*, 98–105. https://doi.org/10.1016/j.colsurfa.2013.03.014.

(59) Augé, G.; Brendlé, J.; Limousy, L.; Thiebault, T. Matériau hybride organique-inorganique apte à adsorber des cations métalliques. FR3078268, August 30, 2019.

TABLE OF CONTENTS

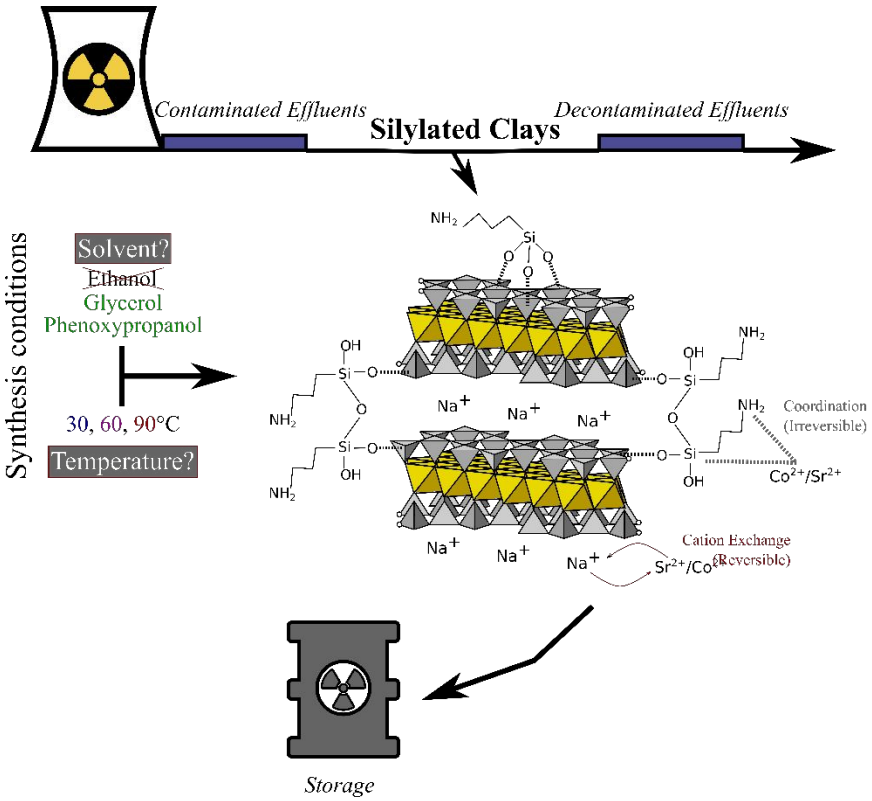
Contaminated Effluents
Silylated Clays
Decontaminated Effluents
Synthesis conditions
Solvent?
Ethanol
Glycerol
Phenoxypropanol
30, 60, 90°C
Temperature?
Coordination
(Irreversible)
Cation Exchange
(Reversible)
Storage